ACS Sustainable Chemistry & Engineering

pubs.acs.org/journal/ascecg

Research Article

Porphyrin Catecholate Iron-Based Metal–Organic Framework for Efficient Visible Light-Promoted One-Pot Tandem C–C Couplings

Saba Daliran, Mostafa Khajeh,* Ali Reza Oveisi,* Hermenegildo García, and Rafael Luque

Cite This: *ACS Sustainable Chem. Eng.* 2022, 10, 5315–5322

Read Online

ACCESS | Metrics & More | Article Recommendations | Supporting Information

ABSTRACT: Introduction of metal–organic frameworks (MOFs) beyond metal-carboxylate series and their applications are still challenging. An innovative porous porphyrin catecholate iron-based MOF (PorphCat-Fe) with a Brunauer–Emmett–Teller (BET) surface area of 700 $m^2 g^{-1}$ has been designed and synthesized through solvothermal self-assembling porphyrin catecholate linkers and iron(II) chloride as a cheap and earth-abundant node precursor. The structure was then evaluated with various techniques and utilized as an efficient and stable heterogeneous material for domino one-pot selective benzyl alcohol oxidation/Knoevenagel condensation reaction under visible LED light irradiation. The photocatalytic performance was remarkably improved as compared to individual components, affording excellent product yields (91%) with almost quantitative transformation of benzyl alcohol. The combination of Fe(III)-Lewis acidic sites and free-base porphyrin photosensitizers within the porous solid material make PorphCat-Fe able to show superior catalytic activity for this transformation. In addition, the MOF can easily accommodate the starting materials inside its mesopores and, thereby, make them easily accessible to active sites. This is an unusual example of an all-in-one noble metal-free bio-inspired supramolecular chemistry for an advanced organic transformation without the need of any chemical additive or further structural modification using only visible LED light conservation.

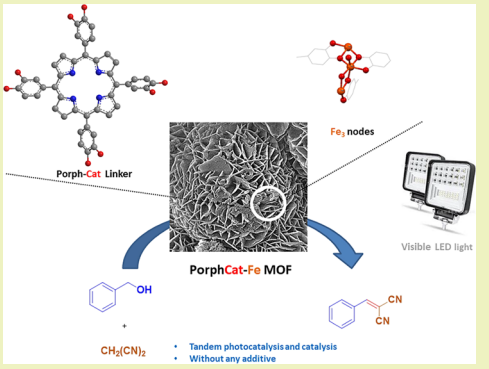

KEYWORDS: *metal–organic frameworks, porphyrin, catechol linker, Fe-based MOF, mesoporous materials, photo-oxidation, cascade reaction, multifunctional catalyst, Knoevenagel reaction*

INTRODUCTION

Metal–organic frameworks (MOFs), three-dimensional (or two-dimensional) crystalline porous coordination polymers, are routinely involved in inorganic metal-containing nodes (secondary building units, SBUs) and multitopic carboxylate organic linkers.[1] The unique properties of MOFs, including high porosity, high surface area, and their high tunable architecture, have delivered new directions for researchers in the chemistry, materials science, engineering, and so on.[1−4]

Porphyrins and their analogues (such as chlorophyll and hemoproteins) are frequently observed in nature,[5] which perform various important biological processes. As a result, they have been enormously investigated in the artificial synthesis and application of porphyrins as attractive materials in different arrays such as drug delivery, medical, electronics, optoelectronics, and photonics.[6,7] However, outside of the biological systems, self-aggregation tendencies and/or self-destructive effects are well-known in porphyrins.[8,9] It has been approved that porphyrin formulation in a porous structure can remarkably stabilize the structure and inhibit the drawbacks mentioned above.

A consecutive combination of multicomponent and multistep synthesis in one-pot reactions, also well-known as tandem/cascade/domino reactions, is a relevant strategy in sustainable and green chemistry in view of waste minimization and energy conservation.[10−14] Recently, some examples of (photo)catalytic conditions containing amino-functionalized MIL-101(Fe),[15] Zr-MOF,[16] Au(III)@Cu(II)-MOF,[17] and Cu-based MOF/TEMPO,[18] have been used for oxidation/Knoevenagel condensation sequential reactions to produce benzylidene derivatives in one-pot reactions. Nevertheless, in spite of successful achievements, the reported protocols suffer from drawbacks including the use of noble metals/oxidant, high voltage UV lamp, excess reagents/substrates, high amount of catalyst and high temperature, as well as the need for postsynthetic modification, which basically restricted their applications. On the other hand, with the increasing global demand for energy, our biggest challenges are the minimization of waste and energy consumption and the efficient use of local clean energy resources. Presently, visible light-active MOF photocatalysts [particularly light-emitting diode (LED)-

Received: February 2, 2022
Revised: March 31, 2022
Published: April 12, 2022

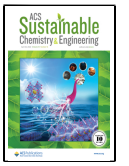

Scheme 1. Schematic for the Synthetic Steps of PorphCat-Fe

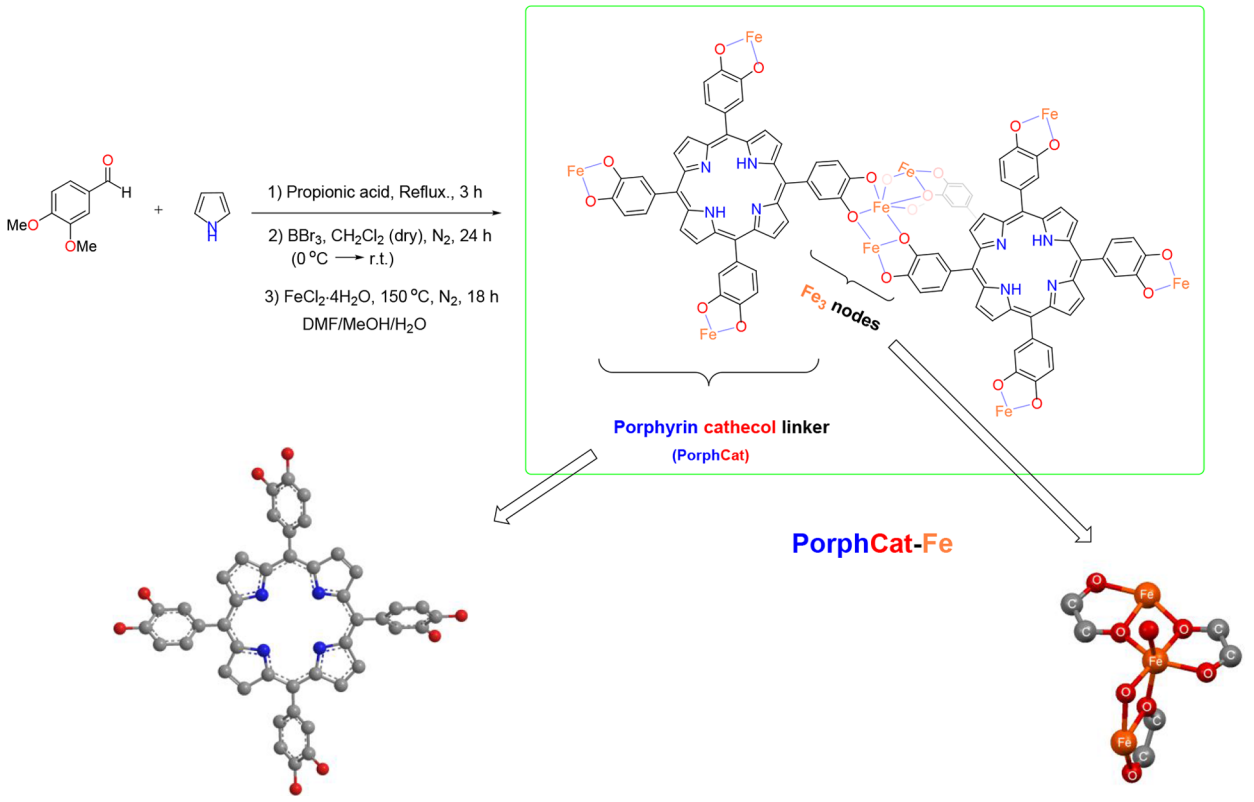

active ones], have been receiving increasing attention in modern organic synthetic procedures to address some of mentioned issues related to waste and energy.[19−21]

Herein, as a proof of concept, we report the synthesis of a mesoporous porphyrin catecholate MOF, denoted here as PorphCat-Fe, through a solvothermal procedure in which the $Fe_3(-C_2O_2-)_6(OH_2)_2$ and the porphyrin catechol linkers are assembled solvothermally in a mixture of DMF/water/methanol. The multifunctional MOF was efficiently used as a new heterogeneous catalyst for sequential one-pot photooxidation of benzyl alcohol/Knoevenagel coupling reaction under visible LED light irradiation and ambient oxygen atmosphere in the absence of any chemical additives. The catalytic activity of the prepared MOF was superior to that of the individual precursors. No obvious loss of activity or catalyst deactivation was observed when the MOF was recovered after reaction. Electron paramagnetic resonance (EPR) measurements and time-resolved phosphorescence allowed for the proposition of a (photo)catalytic mechanism. To the best of our knowledge, this is the first study of such bio-inspired porphyrin catecholate MOF for an organic transformation, which particularly worked under mild conditions without additives.

EXPERIMENTAL SECTION

Materials and Methods. $FeCl_2·4H_2O$, 3,4-dimethoxybenzaldehyde (Veratraldehyde), pyrrole, propionic acid, *N*,*N*′-dimethylformamide (DMF), boron tribromide (BBr_3), CH_3OH, malononitrile, benzyl alcohol, and the used reagents were purchased from Sigma-Aldrich or Merck and used without further purification.

Characterization of MOFs. The MOF was characterized using scanning electron microscopy (TESCAN MIRA3, Czech Republic), energy-dispersive X-ray spectroscopy (EDX), nitrogen adsorption−desorption isotherms (Micromeritics TriStar II 3020 Version 3.02), UV−Vis diffuse reflectance spectroscopy (UV−Vis-DRS, Shimadzu Co., Japan), thermogravimetric analysis (TGA)−differential scanning calorimetry (Mettler-Toledo, Germany), powder X-ray diffraction (PXRD, Bruker D8, Cu Kα irradiation), and Fourier transform infrared spectroscopy (PerkinElmer's Spectrum 100 FT-IR, USA). X-ray photoelectron spectra were recorded on a SPECS spectrometer using a nonmonochromatic X-ray source (Al) working at 200 W. The light exposure was performed by LED lamps (280 power, 3.2 V, 1 W) in a circular holder, ∼32,000 LUX, plus air cooling fans to keep constant the temperature at about 34 °C. Singlet oxygen was studied by time-resolved near-infrared phosphorescence using a homemade set up. Concisely, a pulsed Nd:YAG laser (FTSS355-Q, Crystal Laser) at 355 nm (third harmonic; 0.5 μJ per pulse, 1 kHz repetition rate) was employed for the excitation. An Edmund Optics's notch filter (1064 nm) and an unmodified SKG-5 filter (CVI Laser Corporation) were located at the departure port of the laser. EPR data were obtained on a Bruker EMX (freq. 9.80 GHz, time 80 ms, mofulation freq. 100 kHz). NMR spectra of the products were obtained using a Bruker Avance DPX-250 NMR (300 MHz for ^{1}H and 75 MHz for ^{13}C NMR).

***meso*-Tetrakis-(3,4-dihydroxyphenyl)porphyrin.** The porphyrin (PorphCat) linker was synthesized by a step-wise approach from literature[22,23] as follows: 3,4-dimethoxybenzaldehyde (12 mmol) was dissolved in hot propionic acid (50 mL). Freshly distilled pyrrole (12 mmol, 833 μL) was then added to the reaction mixture before refluxing for 3 h. Upon cooling down the solution, methanol was added and the resulting solid was then filtered and washed with methanol (several times), followed by drying under vacuum to afford *meso*-tetrakis-(3,4-methoxyphenyl)porphyrin product as a dark purple solid (∼12% yield). In the following step, the obtained porphyrin (200 mg) was dissolved in anhydrous dichloromethane (18 mL) at 0 °C under an inert atmosphere before the addition of boron tribromide (0.9 mL, 9.7 mmol) associated with a color change of the solution from deep purple to dark green. After stirring at 0 °C for 1 and 23 h at room temperature under an inert atmosphere, the reaction was quenched with water. The product was then extracted with ethyl acetate and washed with saturated sodium bicarbonate solution and

https://doi.org/10.1021/acssuschemeng.2c00645
ACS Sustainable Chem. Eng. 2022, 10, 5315−5322

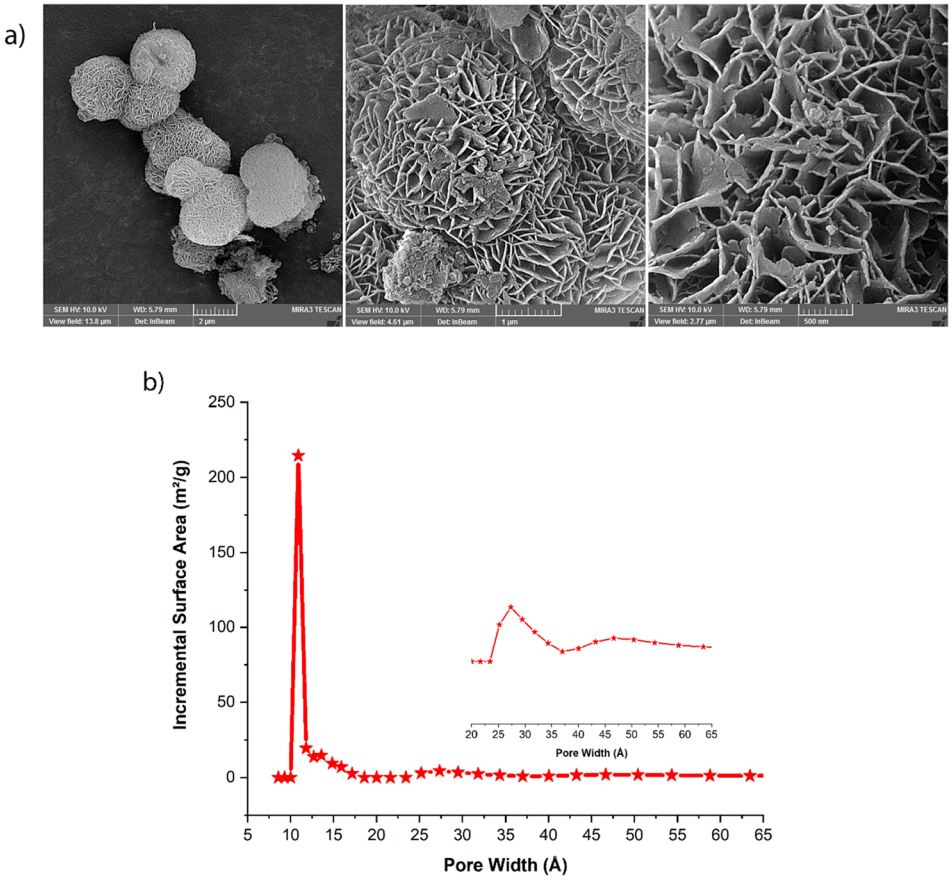

Figure 1. (a) FESEM images with different magnitudes and (b) pore size distribution plots of PorphCat-Fe.

water. The combined organic phases were dried over a drying agent (Na_2SO_4) followed by evaporation of the solvent to give the desired product (PorphCat) as a purple solid (85% yield).

Synthesis of MOF (PorphCat-Fe). In an 18 × 150 mm glass vial, the as-prepared PorphCat (0.0375 mmol) was dissolved in a mixture of DMF/water/methanol (2.5/0.02/0.02 mL) under a N_2 atmosphere. In an independent air-tight vessel, $FeCl_2{\cdot}4H_2O$ (0.15 mmol) was dissolved in 2.5 mL of DMF under N_2. After that, the two solutions were combined together in a sealed tube before being placed in a preheated oven at 150 °C for 18 h. Consequently, the resulting powder was centrifuged and washed with DMF, ethanol, and acetone (twice each). Finally the product was evacuated at 150 °C for 6 h to give the final MOF.

Tandem Photo-Oxidation/Knoevenagel Coupling Procedure. Benzyl alcohol (0.5 mmol) and malononitrile (0.75 mmol) were added to a glass tube including MOF (20 mg) and acetonitrile (~3 mL) equipped with a stir bar. The vial was then connected to an O_2-filled balloon before being illuminated by visible LED lamps. After the completion of the reaction, as monitored by TLC (elution: *n*-hexane/ethyl acetate), the MOF was discharged by centrifugation and solvent was vaporized under vacuum. The pure product was lastly achieved by ethanol−water recrystallization.

RESULTS AND DISCUSSION

Characterization of MOF. This advanced porphyrin catecholate MOF, namely, PorphCat-Fe, consisting of porphyrin catechol, PorphCat, linkers, and Fe_3 nodes, was prepared through self-assembling synthetic PorphCat and iron(II) chloride in a mixed solvent in a preheated oven at 150 °C for 18 h (please see the Experimental Section) (Scheme 1).

Morphology of PorphCat-Fe was established by field emission scanning electron microscopy (FESEM) (Figure 1a). Accordingly, the images revealed a flower-like shape for PorphCat-Fe nanostructures.

Data derived from EDX involve elemental spot (Figure S1) and mapping (Figure S2) of PorphCat-Fe, which confirmed the existence and homogenous distributions of all species including C (50.88 wt %), N (12.43 wt %), O (19.48 wt %), and Fe (16.39 wt %) in the whole structure (Figure S1).

The porosity of the sample was examined via nitrogen physisorption at 77 K. As a result, the BET surface area and pore volume of 700 $m^2\ g^{-1}$ and 0.76 $cm^3\ g^{-1}$, respectively, were correspondingly achieved. The N_2 adsorption−desorption curve presented a typical Type IV/mesoporous isotherm with a hysteresis loop type H3 at around P/P_0 = 0.41−0.99 (Figure S3).

Pore size distribution calculated from the nitrogen adsorption/desorption isotherms using the density functional theory model showed micropores (in the range of 1.0−1.7 nm, centered at ~1.1 nm) and mesopores (in the range of 2.4−3.7 nm, centered at ~2.7, and 4.0−5.8 nm, centered at ~4.7 nm) in the MOF (Figure 1b). The unusual porosity can easily allow for the penetration of guest molecules into the MOF for accessible (photo)catalytic sites.

The thermal stability of the MOF was assessed by using TGA in the temperature range of 25−750 °C under a nitrogen atmosphere. The obtained TGA profile showed that the PorphCat-Fe was thermally stable up to 500 °C with a 65.65% residual weight (Figure S4). The first mass loss occurred before 100 °C was due to removal of adsorbed solvent/

https://doi.org/10.1021/acssuschemeng.2c00645
ACS Sustainable Chem. Eng. 2022, 10, 5315−5322

moisture. The second weight loss between 110 and 280 °C was related to removal of trapped DMF solvent molecules. The next step from ~400 to 750 °C was due to the degradation of the porphyrin linkers and the simultaneously breakdown of the framework.

The DR UV−Vis spectrum of PorphCat-Fe showed the intense adsorption peaks in the visible region, the characteristic Soret and Q bands, which confirmed the presence of the porphyrin linkers in the framework (Figure S5). Band gap energy (E_g) of the PorphCat-Fe was calculated to be 1.55 eV, according to the Tauc plot of $(\alpha h\nu)^{1/2}$ vs photon energy ($h\nu$) (Figure S6),[21] which was promising for visible light photocatalysis.

PorphCat-Fe was examined using PXRD measurement as presented in Figure S7. The PXRD pattern contains the two key diffraction peaks in 2θ values of 6.1° and 8.6°, which are characteristic of the structure (Figure S7). Yaghi and coworkers reported these 2θ values for a similar structure, MOF-1992[Fe]$_3$, albeit by another macrocyclic phthalocyanin-octanol linker, based on the same inorganic SBUs.[24] It should be noted that the compound cannot be obtained like single crystals for single-crystal X-ray diffraction analysis.

Infrared spectra of PorphCat and PorphCat-Fe are shown in Figure S8. The spectra indicated that, after the MOF formation, new peaks at 629 cm^{-1} (Fe−O stretching vibration) and 1005 cm^{-1} (Fe−O bending vibration) are apparently observed, in relation to the strong coordination of oxygen of catecholates of the PorphCat linkers to Fe.

To gain more insights into the MOF structure, X-ray photoelectron spectroscopy (XPS) measurements were consequently performed (Figure 2). Figure 2a−d displays the high

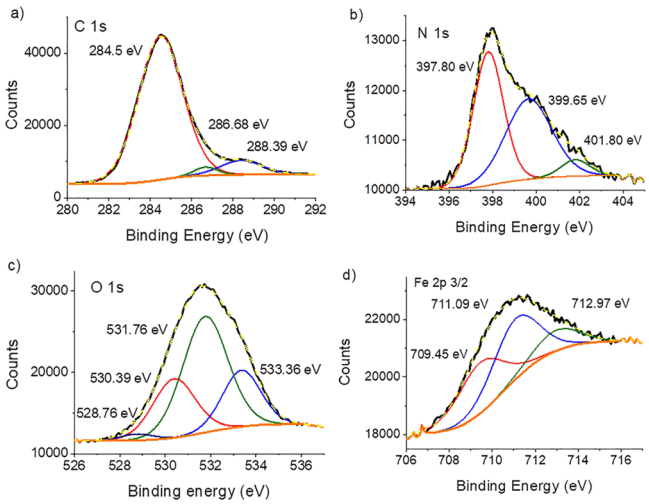

Figure 2. Experimental and fitted XPS spectra of (a) C 1s, (b) N 1s, (c) O 1s, and (d) Fe 2p$_{3/2}$ for PorphCat-Fe MOF.

resolution XPS spectra of the C 1s, N 1s, O 1s, and Fe 2p$_{3/2}$ core levels for PorphCat-Fe, respectively. The high resolution of C 1s region can be deconvoluted into three peaks at 284.5, 286.68, and 288.39 eV.[25] The main peak at 284.5 eV is originated from C═C double bonds of the porphyrin linkers. The peak at 286.68 eV is assigned to C−(O,N) bonds of pyrrol and catecholate rings, and the very weak one at higher binding energies (288.39 eV) is likely due to the presence of C═O groups caused by a partial oxidization of catecholate linkers.[25,26] The N 1s core-level spectrum involves three contributions at 397.80, 399.65, and 401.80 eV.[27,28] The high binding energy peak at 399.65 eV is assigned to pyrrolic N (sp^3 N, 49.0%) and the one at 397.80 eV to the iminic N (sp^2 N, 45.3%).[29] The binding energy at 401.8 eV (5.7%) can be attributed to *N*-oxides. The O 1s core-level spectrum can be fitted to four contributions at 528.76, 530.39, 531.76, and 533.36 eV, corresponding to Fe−O, C−O−Fe, C═O, and O═C−O groups.[30] Fe 2p$_{3/2}$ can be split into three contributions at 709.4, 711.1, and 713.1 eV that can be attributed to Fe−N, Fe−Cl, and mainly Fe^{3+}−O atoms, in good agreement with the structure of PorphCat-Fe.[27,31−33] It also verified that Fe in the PorphCat-Fe existed in the oxidation state of +3.[27]

Photocatalytic Experiments. Benzylidenemalononitriles are of great interest due to their potential applications in pharmaceutical industries.[34] Herein, one-pot tandem selective photo-oxidation of benzyl alcohol/Knoevenagel coupling reaction was considered to assay the catalytic and photocatalytic performance of PorphCat-Fe MOF (Table 1). Interestingly, the reaction between benzyl alcohol and malononitrile in the presence of PorphCat-Fe and visible LED light irradiation in acetonitrile as reaction media afforded 91% yield of benzylidenemalononitrile with quantitative conversion of benzyl alcohol (>99%) after 24 h under an ambient O_2 atmosphere (entry 1, Table 1). However, as given in entry 2, no amount of product was observed without the use of PorphCat-Fe catalyst. In addition, in the absence of light, the reaction with PorphCat-Fe did not proceed nearly to afford target product (entry 3, Table 1). Furthermore, the reaction under the same conditions, nitrogen instead of oxygen, resulted in no desired product formation after 24 h. This result emphasizes the need for PorphCat-Fe, light, and oxygen for the tandem reaction to form benzylidenemalononitrile as the desired product. A slightly lower product yield of 82% was obtained for lower PorphCat-Fe loading in 24 h (entry 5, Table 1). Homogeneous control experiments using the two individual components of PorphCat-Fe ($FeCl_2{\cdot}4H_2O$ and PorphCat) and their physical mixture resulted in no or much lower yields compared to that with PorphCat-Fe under identical conditions (entries 6−8, Table 1). This is due to confinement and stabilization of isolated PorphCat and Fe(III) as photocatalytic and catalytic active centers. Research has shown that homogenous porphyrins are prone to self-degradation and are not stable during (photo)catalytic applications and oxidation reactions. As a heterogeneous solid, combining photocatalysis and catalysis, PorphCat-Fe was filtered out, washed with CH_3CN, dried, and reused in three sequential runs without experiencing a significant loss in activity (entry 1, Table 1). FT-IR and SEM/EDX studies revealed the preservation of the structure of PorphCat-Fe after the photocatalytic reaction (Figures S9 and S10). From XRD analysis results (Figure S11), it was also observed that the catalyst structure remained almost unchanged after reaction. In addition, atomic emission spectroscopy indicated that PorphCat-Fe was stable with a negligible leaching of Fe (~0.2 ppm) into solution. The BET surface area of irradiated PorphCat-Fe was slightly decreased from 700 to ~590 m^2 g^{-1}. The slight reduction might be due to some substrates/intermediates partially blocking the pores. All available data confirmed that PorphCat-Fe is an efficient, stable, and reusable catalyst.

PorphCat-Fe showed superior performance for the light-triggered coupling of benzyl alcohol with malononitrile as

https://doi.org/10.1021/acssuschemeng.2c00645
ACS Sustainable Chem. Eng. 2022, 10, 5315−5322

Table 1. Tandem Selective Photocatalytic Aerobic Oxidation of Benzyl Alcohol/Knoevenagel Coupling Reaction over PorphCat-Fe and Homogeneous Counterparts[a]

entry	catalyst (mg)	O_2/N_2 (1 atm., balloon)	visible LED light	yield (%)[b]
1	PorphCat-Fe (20 mg)	O_2	+	91, 87,[c] 86[d]
2	–	O_2	+	–
3	PorphCat-Fe (20 mg)	O_2	–	trace
4	PorphCat-Fe (20 mg)	N_2	+	–
5	PorphCat-Fe (10 mg)	O_2	+	82
6	PorphCat linker (11 mg)	O_2	+	30
7	$FeCl_2{\cdot}4H_2O$ (26 mg)	O_2	+	–
8	$FeCl_2{\cdot}4H_2O$ (26 mg) + PorphCat linker (11 mg)	O_2	+	47

[a]Reactions were performed using benzyl alcohol (0.5 mmol) and malononitrile (0.7 mmol) in 3 mL of CH_3CN under visible LED light irradiation for 24 h. [b]Isolated product. [c]Second run. [d]Third run.

Table 2. Comparison of the Catalytic Activity over PorphCat-Fe and the Reported (Photo)catalysts in the Literature for the Tandem Coupling Reaction between Benzyl Alcohol and Malononitrile

entry	catalyst (mg)	conditions	solvent	time (h)	conv. (%)	yield (%)	ref.
1	NH_2-MIL-101(Fe) (20 mg)	visible light (300 W Xe), O_2 (1 atm)	$C_6H_5CF_3/CH_3CN$	40	88	72	15
2	Zr-MOF-NH_2 (100 mg)	UV-light irradiation, 90 °C	*p*-xylene	48	100	91	16
3[a]	Au(III)@Cu(II)-MOF (13 mg)	first step: air, 110 °C; second step: r.t.	first step: toluene; second step: toluene/methanol	23	99	>99	17
4[b]	Cu_3TATAT-3 (~68 mg)	TEMPO, 75 °C, O_2 (1 atm)	CH_3CN	12	95	99	18
5	PorphCat-Fe (20 mg)	visible LED light (~34 °C), O_2 (1 atm)	CH_3CN	24	>99	91	this work

[a]Two-step process [b]Cu(II)/amine bifunctional MOF

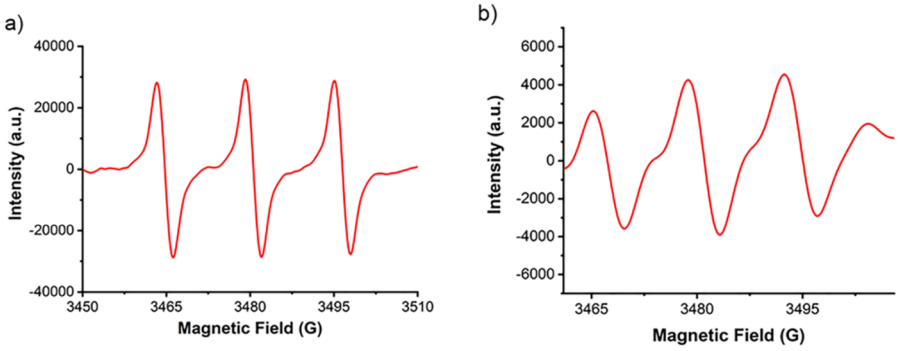

Figure 3. EPR spectra of PorphCat-Fe under visible light irradiation and oxygen atmosphere: (a) TEMP and (b) DMPO.

compared with other reported (photo)catalysts (Table 2). Comparatively, the catalyst could be reused and could lead to the formation of the desired product in excellent yields, and shorter reaction times with quantitative conversion of benzyl alcohol under mild conditions could be achieved by using clean and energy-saving light sources at low catalyst loading without the requirement of any additives or postsynthetic modifications. In addition, in agreement with the concept of "green chemistry," oxygen is inexpensive and produces only water as the byproduct. Furthermore, iron chloride is earth-abundant, cheap, easily accessible, and nontoxic metal precursor. Hence, in this work, we have developed a set of green and sustainable credentials for leading-edge organic chemistry.

Mechanistic Investigations. In order to understand mechanistic pathways in the one-pot sequential photo-oxidation/Knoevenagel coupling reaction, control tests, EPR measurements, and time-resolved phosphorescence were performed. As the model reaction of benzyl alcohol and malononitrile under the standard conditions toward formation of desired product was monitored, benzyl alcohol was selectively (>99%) photo-oxidized to benzaldehyde without any over-oxidation (Scheme S1a). When benzaldehyde was used instead of benzyl alcohol as the staring material, the target product was produced more rapidly (Scheme S1b). These experiments clearly indicate that the reaction using by PorphCat-Fe actually takes place in two key steps: step (I) selective photo-oxidation of benzyl alcohol to benzaldehyde and step (II) Knoevenagel condensation reaction between benzaldehyde (in situ formed) and malononitrile. In addition, the experiments indicated that the nominal tandem reaction is limited mostly by the first step, as it is the slowest one (Scheme S1). Additional control experiments reveal that Fe(III) counterparts can act as typical Lewis acidic sites and PorphCat linkers as both photosensitizers and Lewis basic sites, which all joined together in one component and worked well synergistically (Table 1, entry 4 and Scheme S1c,d). Then, EPR measurements were recorded to detect reactive oxygen species (ROS) formed during the photocatalytic step. By using 2,2,6,6-tetramethylpiperidine (TEMP), as the singlet oxygen ($^1O_2$)

https://doi.org/10.1021/acssuschemeng.2c00645
ACS Sustainable Chem. Eng. 2022, 10, 5315−5322

detection agent, a strong 1:1:1 triplet signal was depicted (Figure 3a), proving $^1O_2$ formation over PorphCat-Fe under the optimum conditions.[35] Strong signals appeared (a quartet, Figure 3b) when 5,5-dimethyl-1-pyrroline *N*-oxide (DMPO) as a superoxide radical anion ($O_2^{\bullet-}$) detection agent was used, indicating that $O_2^{\bullet-}$ species were also formed during the photocatalytic reaction.[21] EPR results obtained obviously pointed out that PorphCat-Fe is capable of generating $^1O_2$ and $O_2^{\bullet-}$ as active oxygen species under visible light irradiation.

To further confirm the generation of reactive $^1O_2$ over PorphCat-Fe, singlet oxygen phosphorescence was directly measured after laser excitation at 355 nm, where it is decayed with a lifetime as high as around 97.47 ns (Figure 4). In addition, it clearly reconfirms the photosensitizer activity of the PorphCat-Fe, benefiting from porphyrin moieties.[36,37]

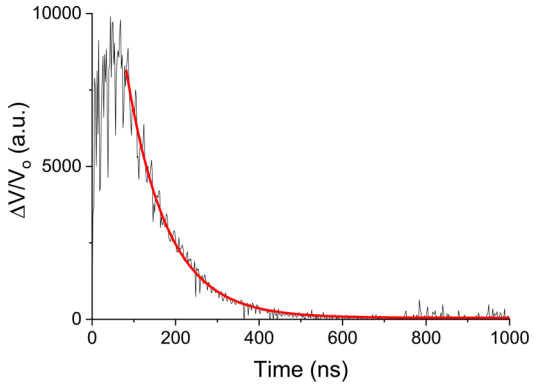

Figure 4. Singlet oxygen phosphorescence upon excitation at 355 nm.

Hereafter, according to a literature survey[15,21,38−40] and obtained results, a probable mechanism for PorphCat-Fe-catalyzed one-pot selective photo-oxidation of benzyl alcohol/Knoevenagel coupling reaction was suggested as depicted in Scheme 2. Upon emission of visible light, PorphCat-Fe adsorbs the light toward generation of the singlet excited state of PorphCat-Fe [PorphCat-Fe*(S1)] and the hole (h^+), which diminishes O_2 into $O_2^{\bullet-}$ by single electron transfer. Also, PorphCat-Fe*(S1) possibly moves into the triplet excited state [PorphCat-Fe*(T1)] by intersystem crossing, which drives O_2 into $^1O_2$ through energy transfer. Concurrently, the hole (h^+) oxidizes benzyl alcohol into benzyl alcohol$^{\bullet+}$ (**A**), which further reacted with formed $O_2^{\bullet-}$ and $^1O_2$ to produce benzaldehyde (**B**). Next, in the presence of Lewis Fe(III)-acidic and basic-porphyrin linker active sites on PorphCat-Fe, the formed aldehyde (**B**) and malononitrile are activated and coupled together to afford the target product (**C**).

CONCLUSIONS

PorphCat-Fe, a Fe MOF based on porphyrin linkers, has been successfully synthesized and completely characterized. PorphCat-Fe features a facile preparation method by using porphyrin containing catechol groups and cost-effective and environment-friendly metal-node precursor, iron(II) chloride. This material remarkably displays mesoporosity with a BET surface area of 700 $m^2\ g^{-1}$ (pore volume 0.76 $cm^3\ g^{-1}$). It is worth revealing that PorphCat-Fe showed outstanding visible light response and combined both heterogenized photocatalysis and catalysis for efficient production of benzylidenemalononitrile via a one-pot green tandem approach without an additive under visible LED irradiation as an energy-saving light source. The photosensitizing and basicity properties of the linker were coupled with the Lewis acidity of Fe-nodes to yield a superior result. In addition, the formation of ROS of $^1O_2$ and $O_2^{\bullet-}$ during the photocatalytic process was evidently confirmed by EPR and phosphorescence techniques. To the best of our knowledge, PorphCat-Fe is the first porphyrin catechol MOF which can open new routes for preparation of MOFs for further applications, particularly for next generation of organic transformations, particularly in view of green and sustainable chemistry.

Scheme 2. Presented Mechanism for One-Pot Tandem (Photo)Catalysis over PorphCat-Fe

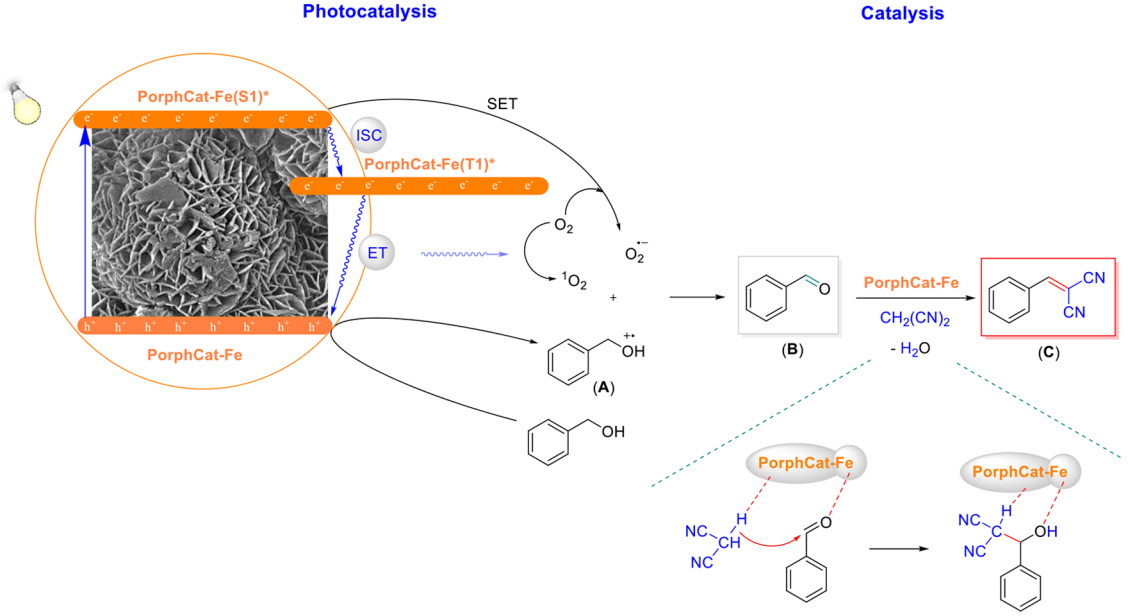

https://doi.org/10.1021/acssuschemeng.2c00645
ACS Sustainable Chem. Eng. 2022, 10, 5315−5322

■ ASSOCIATED CONTENT

Supporting Information

The Supporting Information is available free of charge at https://pubs.acs.org/doi/10.1021/acssuschemeng.2c00645.

SEM images, EDX analyses, TGA profiles, UV−Vis DRS, FT-IR spectra, PXRD patterns, NMR spectra, and control experiments (PDF)

■ AUTHOR INFORMATION

Corresponding Authors

Mostafa Khajeh − *Department of Chemistry, University of Zabol, Zabol 9861335856, Iran*; Email: m_khajeh@uoz.ac.ir

Ali Reza Oveisi − *Department of Chemistry, University of Zabol, Zabol 9861335856, Iran*; orcid.org/0000-0002-0075-211X; Email: aroveisi@uoz.ac.ir

Authors

Saba Daliran − *Department of Chemistry, University of Zabol, Zabol 9861335856, Iran*

Hermenegildo García − *Departamento de Química and Instituto de Tecnología Química CSIC-UPV, Universitat Politècnica de València, Valencia 46022, Spain*; orcid.org/0000-0002-9664-493X

Rafael Luque − *Departamento de Química Orgánica, Universidad de Córdoba, Campus de Rabanales, Edificio Marie Curie (C-3), Cordoba E14014, Spain; Peoples Friendship University of Russia (RUDN University), Moscow 117198, Russia*; orcid.org/0000-0003-4190-1916

Complete contact information is available at: https://pubs.acs.org/10.1021/acssuschemeng.2c00645

Author Contributions

The research was conceived by all the authors. All authors have given approval to the final version of the manuscript.

Notes

The authors declare no competing financial interest.

■ ACKNOWLEDGMENTS

This work was supported by the Iran National Science Foundation (INSF) (Project Number: 98024397). We also thank Monika Kucerakova for assistance with PXRD experiments. The authors wish to acknowledge the University of Zabol (Grant numbers: IR-UOZ-GR-9381). This publication was supported by RUDN University Strategic Academic Leadership Program (R.L.).

■ REFERENCES

(1) Bhadra, B. N.; Ahmed, I.; Lee, H. J.; Jhung, S. H. Metal-organic frameworks bearing free carboxylic acids: Preparation, modification, and applications. *Coord. Chem. Rev.* **2022**, *450*, No. 214237.

(2) Doustkhah, E.; Hassandoost, R.; Khataee, A.; Luque, R.; Assadi, M. H. N. Hard-templated metal−organic frameworks for advanced applications. *Chem. Soc. Rev.* **2021**, *50*, 2927−2953.

(3) Cheung, Y. H.; Ma, K.; van Leeuwen, H. C.; Wasson, M. C.; Wang, X.; Idrees, K. B.; Gong, W.; Cao, R.; Mahle, J. J.; Islamoglu, T.; et al. Immobilized Regenerable Active Chlorine within a Zirconium-Based MOF Textile Composite to Eliminate Biological and Chemical Threats. *J. Am. Chem. Soc.* **2021**, *143*, 16777−16785.

(4) Salcedo-Abraira, P.; Babaryk, A. A.; Montero-Lanzuela, E.; Contreras-Almengor, O. R.; Cabrero-Antonino, M.; Grape, E. S.; Willhammar, T.; Navalón, S.; Elkäim, E.; García, H.; et al. A Novel Porous Ti-Squarate as Efficient Photocatalyst in the Overall Water Splitting Reaction under Simulated Sunlight Irradiation. *Adv. Mater.* **2021**, *33*, No. 2106627.

(5) Lebedeva, N. S.; Gubarev, Y. A.; Koifman, M. O.; Koifman, O. I. The Application of Porphyrins and Their Analogues for Inactivation of Viruses. *Molecules* **2020**, *25*, 4368.

(6) Liu, W.; Lin, C.; Weber, J. A.; Stern, C. L.; Young, R. M.; Wasielewski, M. R.; Stoddart, J. F. Cyclophane-Sustained Ultrastable Porphyrins. *J. Am. Chem. Soc.* **2020**, *142*, 8938−8945.

(7) Massiot, J.; Rosilio, V.; Makky, A. Photo-triggerable liposomal drug delivery systems: from simple porphyrin insertion in the lipid bilayer towards supramolecular assemblies of lipid−porphyrin conjugates. *J. Mater. Chem. B* **2019**, *7*, 1805−1823.

(8) Ding, X.; Wei, S.; Bian, H.; Zhu, L.; Xia, D. Insights into the Self-Aggregation of Porphyrins and Their Influence on Asphaltene Aggregation. *Energy Fuels* **2021**, *35*, 11848−11857.

(9) Wilks, A.; Heinzl, G. Heme oxygenation and the widening paradigm of heme degradation. *Arch. Biochem. Biophys.* **2014**, *544*, 87−95.

(10) Feng, X.; Song, Y.; Lin, W. Dimensional Reduction of Lewis Acidic Metal−Organic Frameworks for Multicomponent Reactions. *J. Am. Chem. Soc.* **2021**, *143*, 8184−8192.

(11) Altuğ, C.; Muñoz-Batista, M. J.; Rodríguez-Padrón, D.; Balu, A. M.; Romero, A. A.; Luque, R. Continuous flow synthesis of amines from the cascade reactions of nitriles and carbonyl-containing compounds promoted by Pt-modified titania catalysts. *Green Chem.* **2019**, *21*, 300−306.

(12) Hao, M.; Li, Z. Visible Light−Initiated Synergistic/Cascade Reactions over Metal−Organic Frameworks. *Sol. RRL* **2021**, *5*, No. 2000454.

(13) Wang, D.; Li, Z. Coupling MOF-based photocatalysis with Pd catalysis over Pd@MIL-100(Fe) for efficient N-alkylation of amines with alcohols under visible light. *J. Catal.* **2016**, *342*, 151−157.

(14) Hao, M.; Li, Z. Efficient visible light initiated one-pot syntheses of secondary amines from nitro aromatics and benzyl alcohols over Pd@NH_2-UiO-66(Zr). *Appl. Catal., B* **2022**, *305*, No. 121031.

(15) Wang, D.; Li, Z. Bi-functional NH_2-MIL-101(Fe) for one-pot tandem photo-oxidation/Knoevenagel condensation between aromatic alcohols and active methylene compounds. *Catal. Sci. Technol.* **2015**, *5*, 1623−1628.

(16) Toyao, T.; Saito, M.; Horiuchi, Y.; Matsuoka, M. Development of a novel one-pot reaction system utilizing a bifunctional Zr-based metal−organic framework. *Catal. Sci. Technol.* **2014**, *4*, 625−628.

(17) Wang, J.-S.; Jin, F.-Z.; Ma, H.-C.; Li, X.-B.; Liu, M.-Y.; Kan, J.-L.; Chen, G.-J.; Dong, Y.-B. Au@Cu(II)-MOF: Highly Efficient Bifunctional Heterogeneous Catalyst for Successive Oxidation−Condensation Reactions. *Inorg. Chem.* **2016**, *55*, 6685−6691.

(18) Miao, Z.; Luan, Y.; Qi, C.; Ramella, D. The synthesis of a bifunctional copper metal organic framework and its application in the aerobic oxidation/Knoevenagel condensation sequential reaction. *Dalton Trans.* **2016**, *45*, 13917−13924.

(19) Dhakshinamoorthy, A.; Li, Z.; Garcia, H. Catalysis and photocatalysis by metal organic frameworks. *Chem. Soc. Rev.* **2018**, *47*, 8134−8172.

(20) Lerma-Berlanga, B.; Ganivet, C. R.; Almora-Barrios, N.; Tatay, S.; Peng, Y.; Albero, J.; Fabelo, O.; González-Platas, J.; García, H.; Padial, N. M.; et al. Effect of Linker Distribution in the Photocatalytic Activity of Multivariate Mesoporous Crystals. *J. Am. Chem. Soc.* **2021**, *143*, 1798−1806.

(21) Karamzadeh, S.; Sanchooli, E.; Oveisi, A. R.; Daliran, S.; Luque, R. Visible-LED-light-driven Photocatalytic Synthesis of N-heterocycles Mediated by A Polyoxometalate-containing Mesoporous Zirconium Metal-organic Framework. *Appl. Catal., B* **2021**, *303*, No. 120815.

(22) Antonangelo, A. R.; Grazia Bezzu, C.; McKeown, N. B.; Nakagaki, S. Highly active manganese porphyrin-based microporous network polymers for selective oxidation reactions. *J. Catal.* **2019**, *369*, 133−142.

(23) Jamaat, P. R.; Davarani, S. S. H.; Fumani, N. S.; Masoumi, L.; Safari, N. A new facile electrochemical method for functionalization of porphyrin. *J. Porphyrins Phthalocyanines* **2008**, *12*, 85−93.
(24) Matheu, R.; Gutierrez-Puebla, E.; Monge, M. Á.; Diercks, C. S.; Kang, J.; Prévot, M. S.; Pei, X.; Hanikel, N.; Zhang, B.; Yang, P.; et al. Three-Dimensional Phthalocyanine Metal-Catecholates for High Electrochemical Carbon Dioxide Reduction. *J. Am. Chem. Soc.* **2019**, *141*, 17081−17085.
(25) Nazri, S.; Khajeh, M.; Oveisi, A. R.; Luque, R.; Rodríguez-Castellón, E.; Ghaffari-Moghaddam, M. Thiol-functionalized PCN-222 MOF for fast and selective extraction of gold ions from aqueous media. *Sep. Purif. Technol.* **2021**, *259*, No. 118197.
(26) Dias, L. D.; Rodrigues, F. M. S.; Calvete, M. J. F.; Carabineiro, S. A. C.; Scherer, M. D.; Caires, A. R. L.; Buijnsters, J. G.; Figueiredo, J. L.; Bagnato, V. S.; Pereira, M. M. Porphyrin−Nanodiamond Hybrid Materials-Active, Stable and Reusable Cyclohexene Oxidation Catalysts. *Catalysts* **2020**, *10*, 1402.
(27) Marshall-Roth, T.; Libretto, N. J.; Wrobel, A. T.; Anderton, K. J.; Pegis, M. L.; Ricke, N. D.; Voorhis, T. V.; Miller, J. T.; Surendranath, Y. A pyridinic Fe-N4 macrocycle models the active sites in Fe/N-doped carbon electrocatalysts. *Nat. Commun.* **2020**, *11*, 5283.
(28) Wechsler, D.; Fernández, C. C.; Köbl, J.; Augustin, L.-M.; Stumm, C.; Jux, N.; Steinrück, H.-P.; Williams, F. J.; Lytken, O. Wet-Chemically Prepared Porphyrin Layers on Rutile TiO(2)(110). *Molecules* **2021**, *26*, 2871.
(29) Diller, K.; Papageorgiou, A. C.; Klappenberger, F.; Allegretti, F.; Barth, J. V.; Auwärter, W. In vacuo interfacial tetrapyrrole metallation. *Chem. Soc. Rev.* **2016**, *45*, 1629−1656.
(30) Li, L.; Ma, P.; Hussain, S.; Jia, L.; Lin, D.; Yin, X.; Lin, Y.; Cheng, Z.; Wang, L. FeS2/carbon hybrids on carbon cloth: a highly efficient and stable counter electrode for dye-sensitized solar cells. *Sustainable Energy Fuels* **2019**, *3*, 1749−1756.
(31) Grosvenor, A. P.; Kobe, B. A.; Biesinger, M. C.; McIntyre, N. S. Investigation of multiplet splitting of Fe 2p XPS spectra and bonding in iron compounds. *Surf. Interface Anal.* **2004**, *36*, 1564−1574.
(32) Momose, Y.; Sakurai, T.; Nakayama, K. Thermal Analysis of Photoelectron Emission (PE) and X-ray Photoelectron Spectroscopy (XPS) Data for Iron Surfaces Scratched in Air, Water, and Liquid Organics. *Appl. Sci.* **2020**, *10*, 2111.
(33) Lv, H.; Zhao, H.; Cao, T.; Qian, L.; Wang, Y.; Zhao, G. Efficient degradation of high concentration azo-dye wastewater by heterogeneous Fenton process with iron-based metal-organic framework. *J. Mol. Catal. A: Chem.* **2015**, *400*, 81−89.
(34) Gazit, A.; Osherov, N.; Posner, I.; Yaish, P.; Poradosu, E.; Gilon, C.; Levitzki, A. Tyrphostins. II. Heterocyclic and .alpha.-substituted benzylidenemalononitrile tyrphostins as potent inhibitors of EGF receptor and ErbB2/neu tyrosine kinases. *J. Med. Chem.* **1991**, *34*, 1896−1907.
(35) Jiang, J.; Liang, Z.; Xiong, X.; Zhou, X.; Ji, H. A Carbazolyl Porphyrin-Based Conjugated Microporous Polymer for Metal-Free Photocatalytic Aerobic Oxidation Reactions. *ChemCatChem* **2020**, *12*, 3523−3529.
(36) Buglak, A. A.; Filatov, M. A.; Hussain, M. A.; Sugimoto, M. Singlet oxygen generation by porphyrins and metalloporphyrins revisited: A quantitative structure-property relationship (QSPR) study. *J. Photochem. Photobiol., A* **2020**, *403*, No. 112833.
(37) Oudi, S.; Oveisi, A. R.; Daliran, S.; Khajeh, M.; Luque, R.; Sen, U.; García, H. Straightforward synthesis of a porous chromium-based porphyrinic metal-organic framework for visible-light triggered selective aerobic oxidation of benzyl alcohol to benzaldehyde. *Appl. Catal., A* **2021**, *611*, No. 117965.
(38) Aziz, A.; Ruiz-Salvador, A. R.; Hernández, N. C.; Calero, S.; Hamad, S.; Grau-Crespo, R. Porphyrin-based metal-organic frameworks for solar fuel synthesis photocatalysis: band gap tuning via iron substitutions. *J. Mater. Chem. A* **2017**, *5*, 11894−11904.
(39) Qin, Y.; Hao, M.; Xu, C.; Li, Z. Visible light initiated oxidative coupling of alcohols and o-phenylenediamines to synthesize benzimidazoles over MIL-101(Fe) promoted by plasmonic Au. *Green Chem.* **2021**, *23*, 4161−4169.
(40) Qian, Y.; Zhang, F.; Pang, H. A Review of MOFs and Their Composites-Based Photocatalysts: Synthesis and Applications. *Adv. Funct. Mater.* **2021**, *31*, No. 2104231.

https://doi.org/10.1021/acssuschemeng.2c00645
ACS Sustainable Chem. Eng. 2022, 10, 5315−5322